Inorg. Chem. **2008**, *47*, 8498−8510

Forum

Structures and Properties of Functional Metal Selenites and Tellurites

Jiang-Gao Mao,* Hai-Long Jiang, and Fang Kong

State Key Laboratory of Structural Chemistry, Fujian Institute of Research on the Structure of Matter, Chinese Academy of Sciences, Fuzhou 350002, People's Republic of China

Received March 28, 2008

Metal selenites and tellurites are a class of very important compounds. In this paper, the structures and properties of metal selenites or tellurites combining with transition-metal (TM) ions with the d^0 electronic configuration or tetrahedral MO_4 building blocks of post-transition main-group elements were reviewed. Most compounds in the alkali or alkaline-earth−d^0 TM−Se^{IV} (or Te^{IV})−O systems exhibit extended anionic architectures composed of distorted octahedra of (d^0) TM cations and tellurite or selenite groups. The distortion of the octahedron is always away from the lone-pair cation, and some of them exhibit excellent second-order nonlinear optical properties due to the adductive effects of two types of bond polarizations. Because of the high coordination number of Ln^{III} ions, most of compounds in the Ln−d^0 TM−Se^{IV} (or Te^{IV})−O systems are not second-harmonic-generation active; however, they are able to emit strong luminescence in the visible or near-IR region; also in most cases, the d^0 TM cations are in tetrahedral geometry and are well separated from selenite or tellurite groups. It is also interesting to note that the selenite group is normally "isolated", whereas the TeO_x ($x = 3-5$) can be polymerized into a variety of discrete polynuclear anionic clusters or extended architectures via Te−O−Te bridges.

Introduction

Noncentrosymmetric (NCS) compounds exhibit many interesting and useful properties such as ferroelectricity, piezoelectricity, and second-order nonlinear optical (NLO) behavior.[1] With inorganic materials, the macroscopic acentricity is often a manifestation of the asymmetric coordination environments of the cations. One of the important classes of NCS compounds is based on cations susceptible to second-order Jahn−Teller (SOJT) distortion.[2] Such a type of distortion can occur in two different types of cations, d^0 transition metals (TMs; Ti^{4+}, V^{5+}, Nb^{5+}, Mo^{6+}, W^{6+}, etc.) and cations with stereoactive lone pairs (Se^{4+}, Te^{4+}, Sb^{3+}, etc.), both in asymmetric coordination environments. With the octahedrally coordinated d^0 TMs, SOJT effects occur when the empty d orbitals of the metal mix with the filled p orbitals of the ligands. In extended structures, this mixing results in a host of nearly degenerate electronic configurations that can be removed through the spontaneous distortion of the d^0 TM.[2] The d^0 TM cation can be distorted toward either a face (local C_3 direction), an edge (local C_2 direction), or a corner (local C_4 direction) of the MO_6 octahedron. The situation with the lone-pair cations is more complex. The structural distortion and polarization was thought to be through the mixing of the metal cation s and p orbitals. Recently, it is believed that the oxide anion also plays an important role in the lone-pair formation. The interaction of the s and p orbitals of the metal cation with the oxide anion p states is critical for lone-pair formation. No matter how the lone pair is created, its structural consequences are profound because the lone pair "pushes" the oxide ligands toward one side of the cation, resulting in a highly asymmetric coordination environment.[3] Studies have shown that compounds containing both types of cations may have a large second-harmonic-generation (SHG) efficiency due to the "constructive" addition of these polarizations, which will be discussed in more detail later.

Tetrahedral groups such as silicates, phosphates, and germanates are very important building units in zeolites and other porous materials that have been widely used as

* To whom correspondence should be addressed. E-mail: mjg@fjirsm.ac.cn.

(1) (a) Wickleder, M. S. *Chem. Rev.* **2002**, *102*, 2011, and references cited therein. (b) Ok, K. M.; Halasyamani, P. S. *Chem. Soc. Rev.* **2006**, *35*, 710. (c) Halasyamani, P.; Peoppelmeier, K. R. *Chem. Mater.* **1998**, *10*, 2753.

(2) (a) Ok, K. M.; Halasyamani, P. S. *Chem. Mater.* **2006**, *18*, 3176. (b) Halasyamani, P. S. *Chem. Mater.* **2004**, *16*, 3586.

(3) (a) Porter, Y.; Bhuvanesh, N. S. P.; Halasyamani, P. S. *Inorg. Chem.* **2001**, *40*, 1172. (b) Porter, Y.; Ok, K. M.; Bhuvanesh, N. S. P.; Halasyamani, P. S. *Chem. Mater.* **2001**, *13*, 1910. (c) Ok, K. M.; Bhuvanesh, N. S. P.; Halasyamani, P. S. *Inorg. Chem.* **2001**, *40*, 1978.

10.1021/ic8005629 CCC: $40.75
Published on Web 09/29/2008

catalysts.[4] Some of phosphates such as KDP (KH_2PO_4) and KTP ($KTiOPO_4$) are also very important second-order NLO materials.[5] Therefore, the combination of these tetrahedral groups with the lone pair containing a Te^{IV} or Se^{IV} cation may also result in new inorganic compounds with novel structural topologies and SHG properties.

It should also pointed out that the transition-metal oxyhalides of Se^{IV} or Te^{IV} display many types of novel structures and interesting magnetic properties such as low-dimensional magnets, etc. Transition-metal tellurium(IV) or selenium(IV) oxyhalides can be regarded as "chemical scissors". The later TM cations form bonds to both oxygen and halide, while lone-pair cations tend to form bonds only to oxygen anions. This chemical difference can be utilized to reduce the dimensionality of the TM arrangements with interesting magnetic properties.[6] It is amazing that many compounds in above systems can be generally formulated as $M_{n+1}(QO_3)_nX_2$, where M, Q, and X represent the TM, Se (or Te), and the halide anion, respectively. Our exploration of the missing members in the nickel system afforded four new compounds, namely, $Ni_{n+1}(QO_3)_nX_2$ (Q = Se, X = Cl, Br, n = 4; Q = Te, X = Cl, n = 6 and 10).[7] We also prepared two new cadmium(II) tellurium(IV) oxychlorides, namely, $\{Cd_2(Te_6O_{13})\}\{Cd_2Cl_6\}$ and $Cd_7Cl_8(Te_7O_{17})$, which display several unusual structural building units: two new types of 1D tellurium(IV) oxide anions ($Te_6O_{13}^{2-}$ and $Te_7O_{17}^{6-}$) (Scheme 1), 1D Cd_2Cl_6 double chains, and 2D Cd_7Cl_8 sheets.[8] We also obtained a series of lanthanide transition-metal tellurium(IV) oxyhalides with three different types of structures, namely, $DyCuTe_2O_6Cl$, $ErCuTe_2O_6Cl$, $ErCuTe_2O_6Br$, $Sm_2Mn(Te_5O_{13})Cl_2$, $Dy_2Cu(Te_5O_{13})Br_2$, and $Nd_4Cu(TeO_3)_5Cl_3$.[9] The halide anion may be involved in metal coordination or remain isolated.

In this paper, our discussion will be focused on only two important systems: combination of Te^{IV} or Se^{IV} with d^0 TMs or with the tetrahedral groups of main-group elements such as SiO_4, GeO_4, BO_4, PO_4, etc. Our group and many other groups have been exploring new NCS compounds in these two systems during the past few years (Table 1). Of course, other Te^{IV} or Se^{IV} compounds are also very important; for example, several good SHG materials have been discovered in compounds with two types of lone-pair cations.[3]

Scheme 1. Selected Examples of Tellurium(IV) Oxide Anions with Polynuclear Cluster Units or Extended Structures

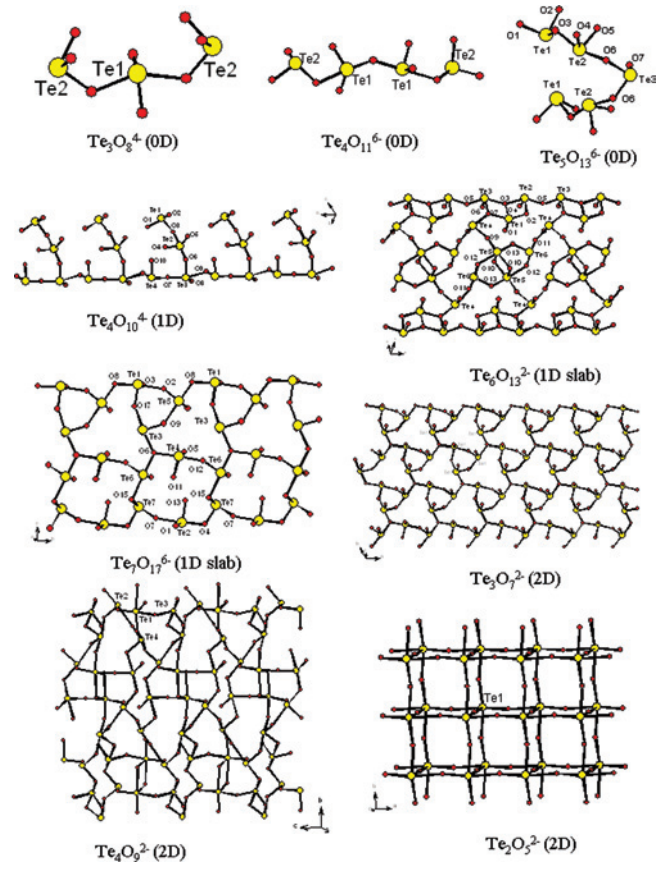

Part I. Combination of d^0 TM Ions with Se^{IV} or Te^{IV}

1. Alkali (or Alkaline Earth)−d^0 TM−Se^{IV} (or Te^{IV})−O System. This system contains a large number of compounds, some of which possess good SHG properties (Table 1). The TM ions with the d^0 electronic configuration are mostly Mo^{6+} and W^{6+}, but there are also some examples involving V^{5+}, Nb^{5+}, and Ta^{5+}.

Five compounds with four different structural types were reported in alkali-metal−molybdenum(VI) selenium(IV) oxide systems A_2MoSeO_6 (A = Na^+, K^+, Rb^+) and $A_2(MoO_3)_3(SeO_3)$ (A = NH_4^+, Cs^+).[10] The first three compounds feature a 3D anionic network, a 0D anionic dimer, and a 1D anionic chain, respectively. The 3D anionic structure of Na_2MoSeO_6 (NCS space group $P2_13$) is based on alternative linkages of MoO_6 octahedra (distorted toward a face) and SeO_3 groups, forming tunnels of Mo_2Se_2 four-membered rings and Mo_4Se_4 eight-membered rings; the sodium cations occupy the larger tunnels. Na_2MoSeO_6 revealed a weak SHG intensity of about 10 × SiO_2. The structure of K_2MoSeO_6 contains two edge-sharing MoO_6 octahedra, each of which is further chelated by a SeO_3 group, forming $[Mo_2Se_2O_{12}]^{4-}$ clusters that are separated by K^+ ions.

(4) (a) Cheetham, A. K.; Férey, G.; Loiseau, T. *Angew. Chem., Int. Ed. Engl.* **1999**, *38*, 3268. (b) Feng, S. H.; Xu, R. R. *Acc. Chem. Res.* **2001**, *34*, 239. (c) Yu, J. H.; Xu, R. R. *Acc. Chem. Res.* **2003**, *36*, 481. (d) Moore, P. B. In *Crystallochemical Aspects of the Phosphate Minerals*; Niagru, J., Moore, P. B., Eds.; Springer-Verlag: Berlin, 1984.
(5) (a) Becker, P. *Adv. Mater.* **1998**, *10*, 979. (b) Chen, C.-T.; Wang, Y.-B.; Wu, B.-C.; Wu, K.-C.; Zeng, W.-L.; Yu, L.-H. *Nature* **1995**, *373*, 322. (c) Chen, C.-T.; Wu, B.-C.; Jiang, A. D.; You, G. M. *Sci. Sin., Ser. B.* **1985**, *28*, 2353. (d) Chen, C.-T.; Wu, Y.; Jiang, A. D.; Wu, B.-C.; You, G.; Li, R.; Lin, S. *J. Opt. Soc. Am. B* **1989**, *6*, 616.
(6) (a) Johnsson, M.; Törnroos, K. W.; Mila, F.; Millet, P. *Chem. Mater.* **2000**, *12*, 2853. (b) Johnsson, M.; Törnroos, K. W.; Lemmens, P.; Millet, P. *Chem. Mater.* **2003**, *15*, 68. (c) Johnsson, M.; Lidin, S.; Törnroos, K. W.; Bürgi, H.-B.; Millet, P. *Angew. Chem., Int. Ed.* **2004**, *43*, 4292. (d) Becker, R.; Johnsson, M.; Kremer, R. K.; Klauss, H.-H.; Lemmens, P. *J. Am. Chem. Soc.* **2006**, *128*, 15469. (e) Becker, R.; Johnsson, M.; Kremer, R.; Lemmens, P. *J. Solid State Chem.* **2005**, *178*, 2024. (f) Millet, P.; Bastide, B.; Johnsson, M. *Solid State Commun.* **2000**, *113*, 719.
(7) (a) Shen, Y.-L.; Mao, J.-G.; Jiang, H.-L. *J. Solid State Chem.* **2005**, *178*, 2942. (b) Jiang, H. L.; Mao, J. G. *Inorg. Chem.* **2006**, *45*, 7593.
(8) Jiang, H. L.; Mao, J. G. *Inorg. Chem.* **2006**, *45*, 717.
(9) Shen, Y. L.; Mao, J. G. *Inorg. Chem.* **2005**, *44*, 5328.
(10) (a) Porter, Y.; Halasyamani, P. S. *J. Solid State Chem.* **2003**, *174*, 441. (b) Harrison, W. T. A.; Dussack, L. L.; Jacobson, A. J. *Inorg. Chem.* **1994**, *33*, 6043.

Table 1. Te^{IV} and Se^{IV} Compounds Showing NCS Structures and SHG Properties

compound	space group	structural feature	SHG efficiency	ref
TeO_2	$P4_12_12$	3D network of corner-sharing TeO_4 groups	5 × SiO_2	3b
Te_2O_5	$P2_1$	3D network of corner-sharing $Te^{4+}O_3$ groups and $Te^{6+}O_6$ octahedra	400 × SiO_2	3b
$TeSeO_4$	Ia	3D network of corner-sharing $Se^{4+}O_3$ and $Te^{4+}O_5$ groups	400 × SiO_2	3a, 3b
Te_2SeO_7	$Pmn2_1$	2D layer composed of $Se^{6+}O_4$ tetrahedra and $Te^{4+}O_4$ groups	200 × SiO_2	3b
Bi_2TeO_5	$Abm2$	3D network of corner-, edge-, or face-sharing BiO_3, BiO_5, and TeO_3 groups	300 × SiO_2	3c
Na_2MoSeO_6	$P2_13$	3D anionic structure based on alternative linkages of MoO_6 octahedra and SeO_3 groups	10 × SiO_2	10a
$Na_2Mo_3Te_3O_{16}$	$I2$	1D chain consisting of Mo_3O_{14} trimers that are connected $Te_3O_8^{4-}$ anions	500 × SiO_2	11a
$(NH_4)_2WTe_2O_8$	$P2_1$	2D layer consisting of WO_6 octahedra connected to TeO_4 polyhedra	250 × SiO_2	12a
$Na_2W_2TeO_9$	Ia	3D structure built from a corrugated 2D tungsten oxide layer further interconnected by TeO_3 groups	500 × SiO_2	12b
$Rb_2W_3TeO_{12}$	$P31c$	2D tungsten oxide layer capped by TeO_3 groups on one side	200 × SiO_2	13b
$Cs_2W_3TeO_{12}$	$P6_3$	2D tungsten oxide layer capped by TeO_3 groups on one side	400 × SiO_2	13b
$BaMo_2TeO_9$	$P2_1$	2D layer built by dimers of edge-sharing MoO_6 octahedra that are interconnected by TeO_3 groups	600 × SiO_2	14b
BaW_2TeO_9	$P2_1$	2D layer built by dimers of edge-sharing WO_6 octahedra that are interconnected by TeO_3 groups	500 × SiO_2	14b
$Cd_4V_2Te_3O_{15}$	$P2_12_12_1$	3D network in which the cadmium tellurite layers are further interconnected by both "isolated" VO_4 tetrahedra and 1D vanadium-oxide helical chains	1.4 × KDP	23
$B_2Se_2O_7$	$P2_12_12_1$	3D network composed of $B_2O_7^{8-}$ anions interconnected by Se^{IV} atoms	2.2 × KDP	27

In Rb_2MoSeO_6, the MoO_6 octahedra are interconnected into a 1D chain via corner-sharing, the SeO_3 groups are hanging on both sides of the chain, and each of them shares an edge with a MoO_6 octahedron.[10a] The last two compounds (space group $P6_3$) are isostructural and feature a 2D hexagonal tungsten bronzelike anionic layer of MoO_6 octahedra capped on one side by pyramidally coordinated Se^{IV};[10b] such a layer was also reported in $Cs_2(MoO_3)_3(TeO_3)$ and $A_2(WO_3)_3(TeO_3)$ (A = Rb, Cs).[11b,12c]

Compounds with three different structural types have been reported in alkali−Mo^{6+}−Te^{4+}−O systems.[11] $Na_2Mo_3Te_3O_{16}$ in NCS space group $I2$ exhibits a quasi-1D crystal structure, with each chain consisting of Mo_3O_{14} trimers (composed of three edge-shared MoO_6 octahedra) that are connected to $Te_3O_8^{4-}$ anions (formed by one TeO_4 group corner-sharing with two TeO_3 groups). Both of the Mo^{6+} and Te^{4+} cations are in the asymmetric coordination environments attributable to SOJT effects. The Mo^{6+} cations are distorted toward an edge of the MoO_6 octahedron (local C_2 direction). The SHG efficiency of $Na_2Mo_3Te_3O_{16}$ is approximately 500 × α-SiO_2 and is phase-matchable. The strong SHG efficiency is maintained up to the melting temperature (around 450 °C).[11a] The use of other alkali-metal ions led to two other structural types.[11b] $A_2Mo_3TeO_{12}$ (A = NH_4, Cs) with noncentrosymmetric space group $P6_3$ contain 2D hexagonal tungsten oxide related $(Mo_3TeO_{12})^{2-}$ anionic layers interleaved with NH_4^+/Cs^+ ions. The TeO_3 groups cap on the same side of the anionic layer. $A_4Mo_6Te_2O_{24}\cdot 6H_2O$ (A = Rb, K) is composed of discrete centrosymmetric $(Mo_6Te_2O_{24})^{4-}$ anionic aggregates and alkali-metal ions. In this hexamolybdoditellurite anion, the Mo_6O_{24} flat hexagonal ring, formed by edge-sharing of six MoO_6 octahedra, is capped by tellurium on both sides. Isolated Mo_6O_{18} and Mo_5O_{15} cyclic clusters capped by SeO_3 groups were also reported with amines as template cations.[13] The Mo^{6+} ions are distorted toward a face of the MoO_6 octahedron in $A_2Mo_3TeO_{12}$ (A = NH_4^+, Cs^+), whereas they are distorted toward an edge in $A_4Mo_6Te_2O_{24}\cdot 6H_2O$ (A = Rb^+, K^+). The Te^{4+} cations in both types of compounds adopt the same asymmetric coordination environments and are bonded to three O atoms.

Three types of compounds were found in the alkali−Te^{IV}−W^{VI}−O systems, namely, $(NH_4)_2WTe_2O_8$, $Na_2W_2TeO_9$, and $A_2W_3TeO_{12}$ (A = K^+, Rb^+, Cs^+).[12] $(NH_4)_2WTe_2O_8$ crystallizes in the noncentrosymmetric (NCS) polar space group $P2_1$ (No. 4). It exhibits a 2D structure consisting of WO_6 octahedra connected to TeO_4 polyhedra; the ammonium cations are located at the interlayer region. Both W^{6+} and Te^{4+} cations are in asymmetric coordination environments attributable to SOJT effects. The WO_6 octahedron exhibits three short and three long W−O bonds. $(NH_4)_2WTe_2O_8$ revealed a moderate SHG efficiency of approximately 250 × α-SiO_2.[12a] The noncentrosymmetric $Na_2W_2TeO_9$ (space group Ia) exhibits a 3D structure comprising distorted WO_6 octahedra linked to asymmetric TeO_3 groups. The WO_6 octahedra form a corrugated 2D tungsten oxide layer through corner-sharing; these layers are further interconnected by TeO_3 groups. Both Te^{IV} and W^{VI} cations are in local acentric environments attributable to SOJT effects. Powder SHG measurements on polycrystalline $Na_2W_2TeO_9$ indicated a strong SHG intensity of approximately 500 × SiO_2, and the material is phase-matchable (type I).[12b] $Cs_2W_3TeO_{12}$ is isostrutural with $Cs_2Mo_3TeO_{12}$.[11b] Although $K_2W_3TeO_{12}$ and $Rb_2W_3TeO_{12}$ have chemical formulas similar to that of $Cs_2W_3TeO_{12}$, their structures are somehow different. All three compounds contain the same

(11) (a) Chi, E. O.; Ok, K. M.; Porter, Y.; Halasyamani, P. S. *Chem. Mater.* **2006**, *18*, 2070. (b) Balraj, V.; Vidyasagar, K. *Inorg. Chem.* **1998**, *37*, 4764.

(12) (a) Kim, J.-H.; Baek, J.; Halasyamani, P. S. *Chem. Mater.* **2007**, *19*, 5637. (b) Goodey, J.; Broussard, J.; Halasyamani, P. S. *Chem. Mater.* **2002**, *14*, 3174. (c) Goodey, J.; Ok, K. M.; Broussard, J.; Hofmann, C.; Escobedo, F. V.; Halasyamani, P. S. *J. Solid State Chem.* **2003**, *175*, 3.

(13) (a) Feng, M.-L.; Mao, J.-G. *Eur. J. Inorg. Chem.* **2004**, 3712. (b) Kortz, U.; Savelieff, M. G.; Ghali, F. Y. A.; Khalil, L. M.; Maalouf, S. M.; Sinno, D. I. *Angew. Chem., Int. Ed.* **2002**, *41*, 4070.

2D tungsten oxide layer of corner-sharing WO_6 octahedra with W_3 and W_6 rings. The TeO_3 groups in $K_2W_3TeO_{12}$ act as interlayer linkers to form a 3D structure. In Rb and Cs compounds, the TeO_3 groups only cap on the same side of the W_3 rings; therefore, the compounds are 2D. The K compound is centrosymmetric, whereas the Rb and Cs compounds are acentric and revealed strong SHG efficiencies of 200 and 400 × SiO_2, respectively. These can be explained by the different radii of the alkali-metal ions; the larger one will have larger interlayer O···O separations, which allows a similar capping of TeO_3 groups and the formation of noncentrosymmetric structures.[12c]

The $AE^{2+}-Mo^{6+}$ (W^{6+})$-Se^{4+}$ (Te^{4+})$-O$ systems are still less explored.[14] Two compounds in the Ba−Mo−Se−O system were reported, $BaMoO_3(SeO_3)$ and $BaMo_2O_5(SeO_3)_2$. $BaMoO_3(SeO_3)$ exhibits a layered structure in which MoO_6 octahedra (distorted toward a face) are bridged by SeO_3 groups, forming Mo_2Se_2 four-membered rings and Mo_3Se_3 six-membered rings. $BaMo_2O_5(SeO_3)_2$ is acentric ($Cmc2_1$) and features a 3D network composed of pairs of corner-sharing MoO_6 octahedra bridged by SeO_3 groups. The MoO_6 octahedron is distorted toward an edge (the local C_2 direction).[14a] $BaMo_2TeO_9$ and BaW_2TeO_9 are isostructural and crystallized in the polar space group $P2_1$; their structures feature an anionic layer composed of MO_6 octahedra linked to the asymmetric TeO_3 polyhedra. The MoO_6 octahedra in $BaMo_2TeO_9$ are distorted toward a face (along the local C_3 [111] direction) with three short and three long Mo−O distances. The WO_6 octahedra in BaW_2TeO_9 exhibit two types of distortion: toward a face as discussed above and toward an edge with two short, two normal, and two long W−O bonds. Two MO_6 octahedra form a dimer via a M−O−M bridge and such dimeric units are further interconnected by TeO_3 groups via M−O−Te bridges. $BaMo_2TeO_9$ and BaW_2TeO_9 revealed extremely strong SHG responses of 600 and 500 × SiO_2, respectively.[14b]

Several phases were reported in $A-V^{5+}-Se^{4+}-O$ systems: $AVSeO_5$ (A = Rb, Cs), $A(VO_2)_3(SeO_3)_2$ (A = K^+, Rb^+, Cs^+, NH_4^+), and the V^{5+}/V^{4+} mixed-valent KV_2SeO_7.[15] $A(VO_2)_3(SeO_3)_2$ (A = K^+, Rb^+, Cs^+, NH_4^+) are isostructural with $A_2(MoO_3)_3(SeO_3)_2$ (A = NH_4^+, Cs^+),[10b] featuring hexagonal layers of corner-sharing VO_6 octahedra, with the SeO_3 groups capping on one side of the vanadium(V) oxide layer; the interlayer distances are much shorter than those of the corresponding Mo compounds because of the much fewer cations needed to balance the charge.[15a,b] The structure of the polar $AVSeO_5$ (A = Rb, Cs; space group $P2_1$) is a 3D anionic network formed by alternative linkages of VO_5 square pyramids and SeO_3 groups via corner-sharing, creating two types of helical tunnels along the *b* axis composed of four- and eight-membered rings. The alkali-metal ions occupy the large tunnels.[15b] KV_2SeO_7 contains both V^{5+} and V^{4+} ions, in octahedral and tetrahedral coordination environments, respectively. Its structure features a double layer of $\{V_2SeO_7\}^-$ composed of corner-sharing VO_6 octahedra, VO_4 tetrahedra, and SeO_3 groups.[15c]

Only one compound was reported for the alkaline earth$-V^{V}-Se^{IV}-O$ family. $Ba_{2.5}(VO_2)_3(SeO_3)_4 \cdot H_2O$ exhibits a 2D-layered structure consisting of layers of VO_5 square pyramids linked to SeO_3 polyhedra, with the Ba^{2+} cations and water molecules occupying the interlayer region.[16] Each layer consists of eclipsed 12-membered V_6Se_6 rings and smaller eight-membered V_4Se_4 rings. Each V^{5+} is bonded to five O atoms in a distorted square-pyramidal environment with two "short" [1.642(9) and 1.647(9) Å] and three "normal" bonds [1.952-(8)−2.006(9) Å]. Three of the five O atoms are further bonded to Se^{4+} cations, whereas the two "short" V−O bonds remain terminal. The selenite groups adopt two types of binding modes: tridentate bridging with three Se−O−V bridges and bidentate with only two Se−O−V bridges.

Reports on $A(Ae)-Nb^{5+}$ (or Ta^{5+})$-Se^{4+}$ (or Te^{4+})$-O$ systems are still rare.[17] The structural backbone of $Na_{1.4}Nb_3Te_{4.9}O_{18}$ may be considered as two sets of corner-shared NbO_6 octahedral chains. The "first" chain consists of one row of corner-shared NbO_6 octahedra that are linked by TeO_3 and TeO_4 polyhedra, whereas the "second" chain consists of two rows of corner-shared NbO_6 octahedra that are linked by TeO_3 groups. Each of these chains of octahedra runs parallel to the [010] direction. The "first" and "second" chains are linked by the TeO_3 and TeO_4 groups, along the [100] and [010] directions, resulting in the 3D topology. The Te^{4+} cation that connects the two chains is partially occupied. The Na^+ cations reside in the spaces between the two chains. The second compound, $NaNb_3Te_4O_{16}$, also exhibits a 3D structure consisting of corner-linked NbO_6 octahedra that are connected to asymmetric TeO_3 and TeO_4 groups. Similar to $Na_{1.4}Nb_3Te_{4.9}O_{18}$, the structural backbone of $NaNb_3Te_4O_{16}$ may also be considered as an infinite chain of corner-shared NbO_6 octahedra. The chain consists of three corner-shared NbO_6 octahedra running along the [001] direction. These octahedra are infinite, through additional corner-sharing, in the [010] direction. The TeO_3 and TeO_4 groups serve to link these NbO_6 octahedra. The Na^+ cations reside in the spaces between the NbO_6 octahedra. In both compounds, the distortion of the NbO_6 octahedron is along the local C_4 direction.[17a] The crystal structures of $Ba_2M_6Te_2O_{21}$ (M = Nb, Ta) are dominated by the $[M_6O_{21}]^{12-}$ anionic network with incorporated Ba^{2+} and Te^{4+} ions. Tunnels based on M_4, M_3Te and M_6Te_2 rings are formed along the [010] direction; the Ba^{2+} ions occupy the tunnels of eight-membered rings.[17b]

2. Ln−d^0 TM−Te^{IV} or Se^{IV}−O Systems. Only three compounds, namely, $LaNbTeO_6$ and $La_4M_2Te_6O_{23}$ (M = Nb, Ta), were reported by the Halasyamani group before our group's work on this research field.[18] $LaNbTeO_6$ consists of 1D corner-linked chains of NbO_6 octahedra that are

(14) (a) Harrison, W. T. A.; Dussack, L. L.; Jacobson, A. J. *J. Solid. State Chem.* **1996**, *125*, 234. (b) Ra, H. S.; Ok, K. M.; Halasyamani, P. S. *J. Am. Chem. Soc.* **2003**, *125*, 7764.

(15) (a) Vaughey, J.-T.; Harrison, W. T. A.; Dussack, L. L.; Jacobson, A. J. *Inorg. Chem.* **1994**, *33*, 4370. (b) Kwon, Y.-U.; Lee, K.-S.; Kim, Y.-H. *Inorg. Chem.* **1996**, *35*, 1161. (c) Lee, K.-S.; Kwon, Y.-U.; Namgung, H.; Kim, S.-W. *Inorg. Chem.* **1995**, *34*, 4178.

(16) Sivakumar, T.; Ok, K. M.; Halasyamani, P. S. *Inorg. Chem.* **2006**, *45*, 3602.

(17) (a) Ok, K. M.; Halasyamani, P. S. *Inorg. Chem.* **2005**, *44*, 3919. (b) Muller-Buschbaum, H.; Wedel, B. *Z. Naturforsch.* **1996**, *51*, 1411.

connected by TeO_3 polyhedra. $La_4M_2Te_6O_{23}$ (M = Nb, Ta) also has a 1D crystal structure, consisting of different types of chains that run parallel to the *c* axis. One chain consists of corner-linked MO_6 octahedra. Each MO_6 octahedron shares additional corners with TeO_3 and TeO_4 groups. The TeO_3 polyhedra are separated from each other, but the TeO_4 groups are connected through an O atom into the TeO_4 "chain", which is broken at random intervals because of the defects on the bridging O atoms. The other chain is the isolated TeO_4 chain that is also broken at random intervals because of the defects. In all three compounds, the Nb^{5+} or Ta^{5+} cation is distorted toward an edge with two "short", two "normal", and two long $M^{5+}-O$ bonds; the short ones are terminal and the long ones are connected to a Te^{4+} cation, whereas the remaining two bonds are involved in the $M^{5+}-O-M^{5+}$ bridges. In all three compounds, Te^{4+} cation is in an asymmetric coordination environment attributable to its stereoactive lone pair.

We think that a slight change of the radius of the Ln^{III} ion may induce a completely different structure; in other words, the "lanthanide contraction" may play an important role in the structures formed. Furthermore, lanthanide compounds are capable of emitting strong luminescence in the visible and near-IR regions; both oxyanions of d^0 TM and Te^{IV} (or Se^{IV}) are good activators for luminescence of the Ln^{III} ions. Like corresponding alkali or alkaline-earth compounds, Ln^{III} compounds with NCS structures may also be formed. Therefore, systematic investigation of the lanthanide selenium(IV) or tellurium(IV) oxides with additional TM ions with a d^0 electronic configuration may give rise to new lanthanide NLO materials or luminescent materials. Solid-state reactions of lanthanide(III) oxide (and/or lanthanide(III) oxychloride), MoO_3 (or WO_3) and TeO_2 at high temperature led to 12 new compounds with 8 different types of structures, namely, $Nd_2MoSe_2O_{10}$, $Gd_2MoSe_3O_{12}$, $La_2MoTe_3O_{12}$, $Nd_2MoTe_3O_{12}$, $Ln_2MoTe_4O_{14}$ (Ln = Pr, Nd), $La_2WTe_6O_{18}$, $Nd_2W_2Te_2O_{13}$, and $Ln_5MTe_7O_{23}Cl_3$ (Ln = Pr, Nd; M = Mo, W).[19]

$Nd_2MoSe_2O_{10}$ can also be formulated as $Nd_2(MoO_4)(SeO_3)_2$. Its structure features a 3D network in which the Nd^{III} ions are interconnected by SeO_3^{2-} anions and MoO_4 tetrahedra (Figure 1). Both Nd1 and Nd2 are eight-coordinated by eight O atoms with Nd−O distances in the range of 2.407(7)−2.540(7) Å. The Mo^{VI} atom is in a slightly distorted tetrahedral coordination environment with Mo−O distances in the range of 1.740(7)−1.816(6) Å. The interconnection of Nd1 atoms via bridging selenite groups leads to a ⟨001⟩ layer, whereas Nd2 atoms are bridged by MoO_4 tetrahedra to form a ⟨002⟩ layer. The above two types of layers are further interconnected via Nd−O−Se bridges into a 3D network (Figure 1). The lone pairs of the Se^{IV} cations are oriented toward the cavities of the structure.

When the molar ratio of Se/Ln was increased to 3:2, $Gd_2MoSe_3O_{12}$ with a different structure was obtained.

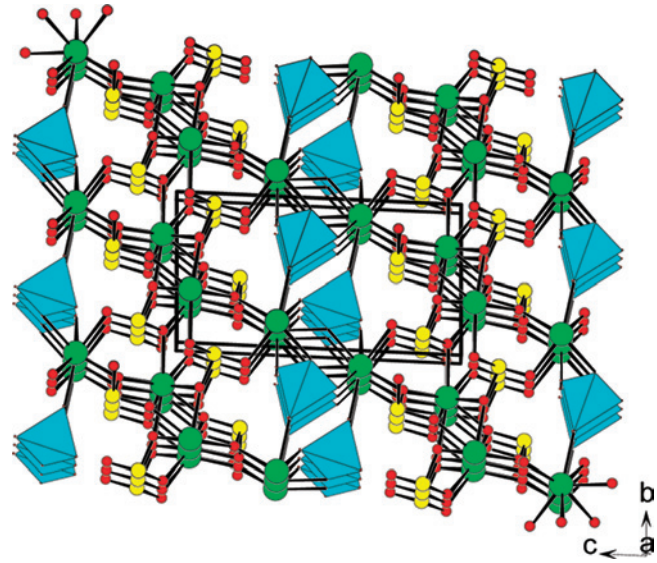

Figure 1. View of the structure of $Nd_2MoSe_2O_{10}$ down the *a* axis. The MoO_4 tetrahedra are shaded in cyan. Nd, Se, and O atoms are drawn as green, yellow, and red circles, respectively.

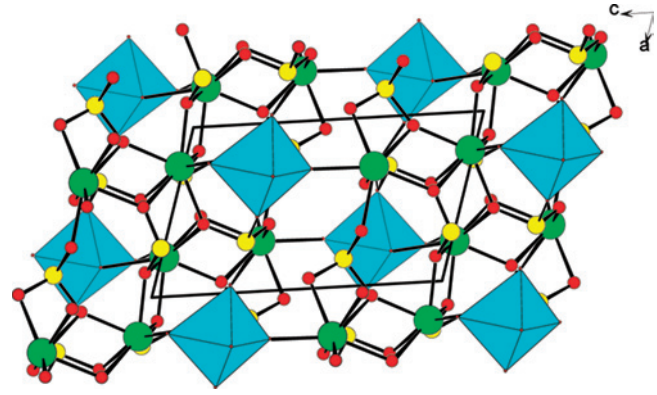

Figure 2. View of the structure of $Gd_2MoSe_3O_{12}$ down the *b* axis. The MoO_6 tetrahedra are shaded in cyan. Gd, Se, and O atoms are drawn as green, yellow, and red circles, respectively.

$Gd_2MoSe_3O_{12}$ can also be formulated as $Gd_2(MoO_3)(SeO_3)_3$, which can be considered as one O^{2-} anion of $Nd_2MoSe_2O_{10}$ being replaced by the third selenite group. The structure of $Gd_2MoSe_3O_{12}$ features a 3D network of gadolinium(III) selenite, with the MoO_6 octahedra occupying the cavities of the network. Both Gd atoms in the asymmetric unit are eight-coordinated, with Gd−O distances ranging from 2.337(5) to 2.485(5) Å. Unlike that in $Nd_2MoSe_2O_{10}$, the Mo^{VI} atom in $Gd_2MoSe_3O_{12}$ is octahedrally coordinated by three O atoms from three selenite groups and three O^{2-} anions (Figure 2). The MoO_6 octahedron is distorted toward a face (local C_3 direction), exhibiting three "long" and three "short" Mo−O bonds. The magnitude of the distortion (Δ_d) is 1.492. The interconnection of the Gd^{III} ions by selenite groups results in a 3D network with tunnels running along the *b* axis. The MoO_6 octahedra are located at the tunnels formed by gadolinium(III) selenite (Figure 2).

The structure of $La_2MoTe_3O_{12}$ is composed of two La^{3+} ions, one MoO_4^{2-} anion, and one $Te_3O_8^{4-}$ anion. It can be considered as two selenite groups in $Nd_2MoSe_2O_{10}$ being replaced by a $Te_3O_8^{4-}$ anion. The La^{3+} ion is nine-coordinated by seven O atoms from four $Te_3O_8^{4-}$ anions and

(18) Ok, K. M.; Zhang, L.; Halasyamani, P. S. *J. Solid State Chem.* **2003**, *175*, 264.
(19) (a) Shen, Y. L.; Jiang, H. L.; Xu, J.; Mao, J. G.; Cheah, K. W. *Inorg. Chem.* **2005**, *44*, 9314. (b) Jiang, H. L.; Ma, E.; Mao, J. G. *Inorg. Chem.* **2007**, *46*, 7012.

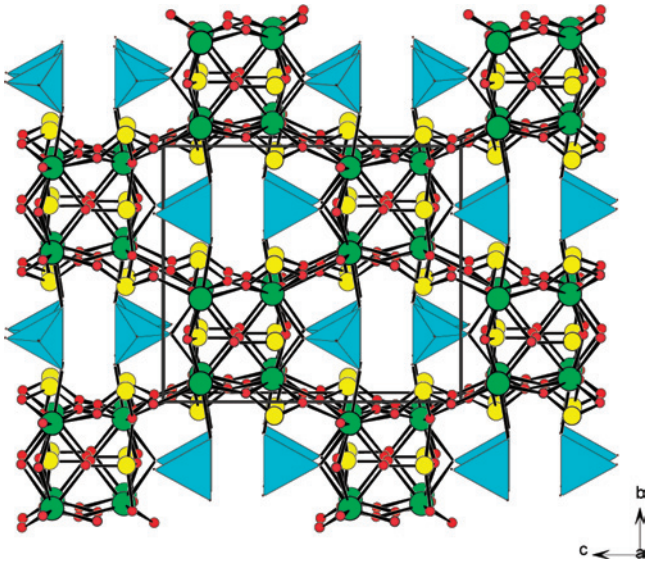

Figure 3. View of the structure of $La_2MoO_4(Te_3O_8)$ down the *a* axis. The MoO_4 tetrahedra are shaded in cyan. La, Te, and O atoms are drawn as green, yellow, and red circles, respectively.

two O atoms from two MoO_4^{2-} anions. The La−O distances range from 2.451(8) to 2.821(8) Å. The trinuclear $Te_3O_8^{4-}$ anion is formed by one TeO_4 group corner-sharing with two TeO_3 groups. The Mo^{VI} cation is in a slightly distorted tetrahedral coordination geometry, with the Mo−O distances ranging from 1.754(8) to 1.793(11) Å. The interconnection of the La^{3+} by chelating and bridging $Te_3O_8^{4-}$ anions led to a 3D network with tunnels along the *a* axis. These tunnels are formed by 10-membered rings (six La and four Te). The MoO_4 polyhedra are located at the above tunnels and connected with the La^{3+} ions via corner-sharing (Figure 3).

$Nd_2MoTe_3O_{12}$ can be formulated as $Nd_2(MoO_4)(TeO_3)(Te_2O_5)$; it can also be considered as the $Te_3O_8^{4-}$ anion in $La_2MoTe_3O_{12}$ being replaced by a tellurite and a ditellurite group. Different from the La^{3+} ion in $La_2MoO_4(Te_3O_8)$, the Nd^{III} ion in $Nd_2(MoO_4)(TeO_3)(Te_2O_5)$ is eight-coordinated by eight O atoms, with the Nd−O distances in the range of 2.324(4)−2.603(4) Å. The Te^{IV} cations of the tellurite and ditellurite groups are coordinated by three O atoms in an asymmetric environment. The Te−O distances are in the range of 1.838(4)−1.987(2) Å. The interconnection of Nd^{III} ions by bridging tellurite and ditellurite groups afforded a layered architecture (Figure 4). The MoO_4 tetrahedron was capped on four Nd^{III} ions of the 2D layer with the terminal O1 atom toward the interlayer space (Figure 4). The interlayer distance is about 8.85 Å.[19a]

The use of more TeO_2 in the syntheses led to $Ln_2MoTe_4O_{14}$ (Ln = Pr, Nd). Both compounds are isostructural and feature a 3D network in which the Ln^{III} ions are interconnected by 1D $Te_4O_{10}^{4-}$ chains and MoO_4 tetrahedra (Figure 5). Therefore, $Ln_2MoTe_4O_{14}$ (Ln = Pr, Nd) can also be formulated as $Ln_2(MoO_4)(Te_4O_{10})$ (Ln = Pr, Nd). Among two unique Ln^{III} atoms in the asymmetric unit, one is eight-coordinated by eight tellurite O atoms whereas the other is eight-coordinated by six tellurite O atoms and two O atoms from two molybdate anions. The Mo^{VI} atom is in a slightly distorted tetrahedral coordination environment with Mo−O

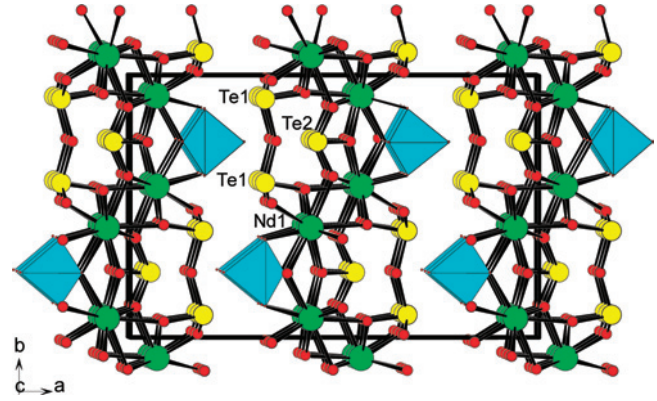

Figure 4. View of the structure of $Nd_2(MoO_4)(TeO_3)(Te_2O_5)$ down the *c* axis. The MoO_4 tetrahedra are shaded in cyan. Nd, Te, and O atoms are drawn as green, yellow, and red circles, respectively.

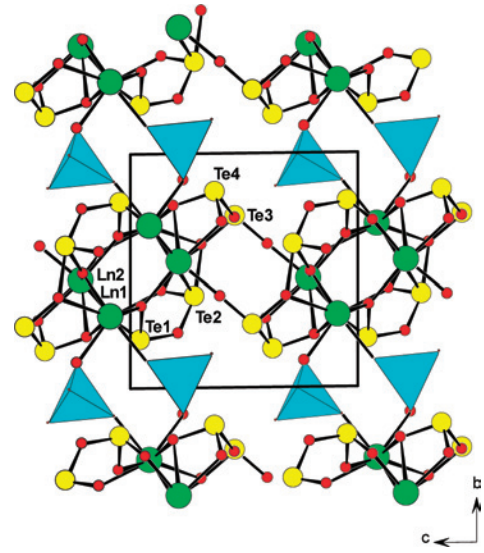

Figure 5. View of the structure of $Ln_2MoTe_4O_{14}$ down *a*-axis. The MoO_4 tetrahedra are shaded in cyan. Ln, Te, and O atoms are drawn as green, yellow, and red circles, respectively.

distances in the range of 1.733(4)−1.779(4) Å. The Te^{IV} atoms are three- or four-coordinated by O atoms in an asymmetric environment. The Te−O distances are in the range of 1.826(3)−2.457(3) Å. The TeO_3 and TeO_4 groups are interconnected via corner-sharing into a novel 1D $Te_4O_{10}^{4-}$ anionic chain (Scheme 1). The interconnection of Nd1 and Nd2 atoms via bridging $Te_4O_{10}^{4-}$ anionic chains led to neodymium(III) tellurium(IV) oxide layers, which are further interconnected by MoO_4 tetrahedra into a 3D network with apertures along the *a* axis. The aperture is formed by 10-membered rings containing six Ln^{III} ions, two MoO_4^{2-} anions, and two TeO_4 groups. The lone pairs of the Te^{IV} atoms are oriented toward the apertures of the structure (Figure 5). It is worth comparing the structures of $Ln_2MoTe_4O_{14}$ (Ln = Pr, Nd) with those of $La_2MoTe_3O_{12}$ and $Nd_2MoTe_3O_{12}$. All four compounds contain MoO_4 tetrahedra; however, their Te−O architectures are completely different: $La_2MoTe_3O_{12}$ features discrete $Te_3O_8^{4-}$ anions, whereas $Nd_2MoTe_3O_{12}$ contains both TeO_3^{2-} and dimeric $Te_2O_5^{2-}$ anions, and 1D $Te_4O_{10}^{4-}$ anions are formed in $Ln_2MoTe_4O_{14}$ (Ln = Pr, Nd). $Nd_2MoTe_3O_{12}$ features a layered structure with MoO_4 tetrahedra hanging between two

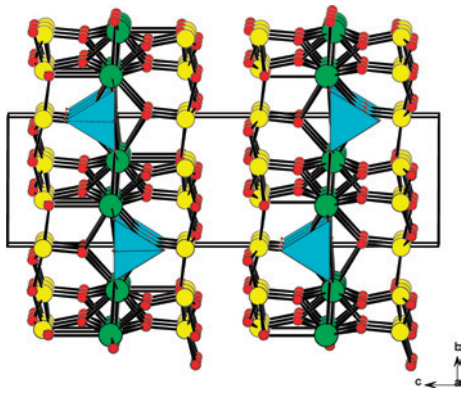

Figure 6. View of the structure of $La_2WTe_6O_{18}$ down the *a* axis. The WO_4 tetrahedra are shaded in cyan. La, Te, and O atoms are drawn as green, yellow, and red circles, respectively.

neighboring layers, whereas the MoO_4 tetrahedra in $La_2MoTe_3O_{12}$ are located at the tunnels of lanthanum(III) tellurium(IV) oxide. In $Ln_2MoTe_4O_{14}$ (Ln = Pr, Nd), the MoO_4 tetrahedron serves as a bridge between two lanthanide(III) tellurium(IV) oxide layers.

The above synthetic methods were also applied to the $Ln^{III}-W^{VI}-Te^{IV}-O$ systems. $La_2WTe_6O_{18}$ was obtained when we attempted to prepare the W^{VI} analogue of $La_2MoTe_3O_{12}$. $La_2WTe_6O_{18}$ can also be formulated as $La_2(WO_4)(Te_3O_7)_2$. The La1 atom is 10-coordinated by seven O atoms from two $Te_3O_7^{2-}$ anions and three O atoms from three WO_4 tetrahedra. The La−O distances range from 2.487(4) to 2.884(8) Å. The W^{VI} atom is tetrahedrally coordinated by four O atoms, with the W−O distances ranging from 1.724(6) to 1.786(1) Å. The Te^{IV} atom is coordinated by four O atoms with Te−O distances in the range of 1.850(4)−2.193(1) Å. The TeO_4 groups are interconnected into a $Te_3O_7^{2-}$ layer via corner-sharing (Scheme 1). Within the layer, three-membered rings and "pear-shaped" six-membered rings are found. Similar Te_3 and "pear-shaped" Te_6 rings have been reported in $Cd_7Cl_8(Te_7O_{17})$.[8] The interconnection of La^{3+} ions by bridging WO_4^{2-} anions led to a 2D $[La_2WO_4]^{4+}$ layer along the *ab* plane. One $[La_2WO_4]^{4+}$ layer and two $Te_3O_7^{2-}$ layers are further interconnected into a thick layer in the *ab* plane via La−O−Te bridges (Figure 6). The thickness of the layer is about 7.65 Å, and the interlayer opening width is about 3.0 Å. This type of layer can also be viewed as the $[La_2WO_4]^{4+}$ layer being sandwiched between two $Te_3O_7^{2-}$ anionic layers. The lone-pair electrons of Te^{IV} atoms are oriented toward the interlayer space (Figure 6).

$Nd_2W_2Te_2O_{13}$ with a different structure was obtained in our attempts to prepare the Nd^{III} analogue of $La_2WTe_6O_{18}$. $Nd_2W_2Te_2O_{13}$ features a 3D network structure in which the W_2O_{10} dimers occupy the large apertures formed by neodymium tellurite (Figure 7). Among two unique Nd^{3+} ions in the asymmetric unit, one is eight-coordinated whereas the other one is nine-coordinated. The Nd−O distances range from 2.333(5) to 2.681(5) Å. Unlike that in $La_2WTe_6O_{18}$, both of the W^{VI} cations in $Nd_2W_2Te_2O_{13}$ are octahedrally coordinated. W1 is coordinated by two O atoms from two tellurite groups and four terminal O atoms, whereas W2 is coordinated by one O atom from a tellurite group and five

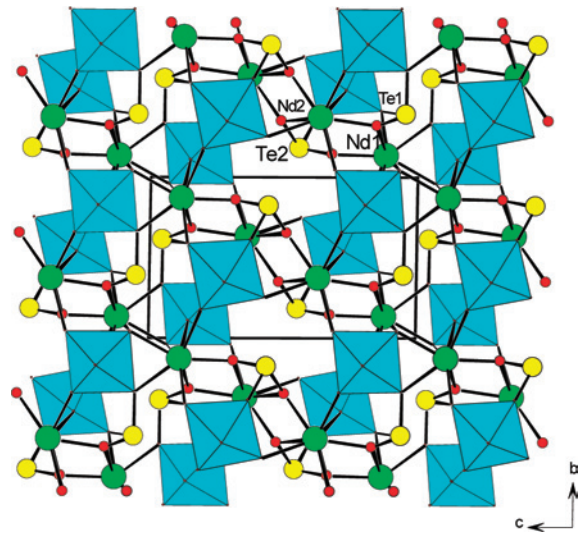

Figure 7. View of the structure of $Nd_2W_2Te_2O_{13}$ down the *a* axis. The WO_4 tetrahedra are shaded in cyan. Nd, Te, and O atoms are drawn as green, yellow, and red circles, respectively.

terminal O atoms. A pair of WO_6 octahedra is interconnected via edge-sharing into a $W_2O_{10}^{8-}$ dimer. Both of the WO_6 octahedra are severely distorted. The W1 atom is distorted toward a face (local C_3 direction) with three "short" [1.743(6)−1.834(5) Å] and three "long" [2.033(5)−2.300(5) Å] W−O bonds, whereas the W2 atom is distorted toward an edge (C_2) with two "short" [1.747(5) and 1.767(5) Å], two "normal" [1.900(5) and 1.930(5) Å], and two "long" [2.172(5) and 2.232(5) Å] W−O bonds. Again both W^{VI} cations are distorted away from the O atoms that bonded to the Te^{4+} cations. The magnitudes of the distortion (Δ_d) are 1.118 and 0.945 Å respectively for $W1O_6$ and $W2O_6$. The interconnection of the Nd^{III} ions by the tellurite groups resulted in a 3D network with two types of apertures along the *a* axis (Figure 7). The large apertures with a narrow-long shape are formed by 10-membered rings composed by four TeO_3 groups and six Nd^{III} ions, and the small ones are formed by four-membered rings composed of two Nd1 and two $Te1O_3$ groups. The W_2O_{10} dimers are located at the large apertures (Figure 7). In $Nd_2W_2Te_2O_{13}$, each W_2O_{10} dimer connects with two TeO_3 groups (one in a unidentate fashion, and the other in a bidentate bridging fashion) to form a $[W_2Te_2O_{13}]^{6-}$ anion. Therefore, the structure of $Nd_2W_2Te_2O_{13}$ also can be viewed as the Nd^{3+} ions being interconnected by $[W_2Te_2O_{13}]^{6-}$ anions via Nd−O−Te and Nd−O−W bridges (Figure 7).

When chloride anion was introduced into the Ln−Mo (W)−Te−O system, isostructural $Ln_5MTe_7O_{23}Cl_3$ (Ln = Pr, Nd; M = Mo, W) were obtained. These compounds feature a 3D network of a lanthanide(III) molybdenum(VI) tellurium(IV) oxychloride with large apertures occupied by isolated Cl anions and the lone-pair electrons of Te^{IV} (Figure 8). $Ln_5MTe_7O_{23}Cl_3$ can also be formulated as $Ln_5(MO_4)(Te_5O_{13})(TeO_3)_2Cl_3$. The asymmetric unit of $Ln_5MoTe_7O_{23}Cl_3$ contains three unique Ln^{III} ions, one M^{VI} cation, and four Te atoms. Two Ln^{III} ions are 8-coordinated, whereas the third one is 10-coordinated. The Ln−Cl distances are significantly longer than those of the Ln−O bonds. The M^{VI} cation is in

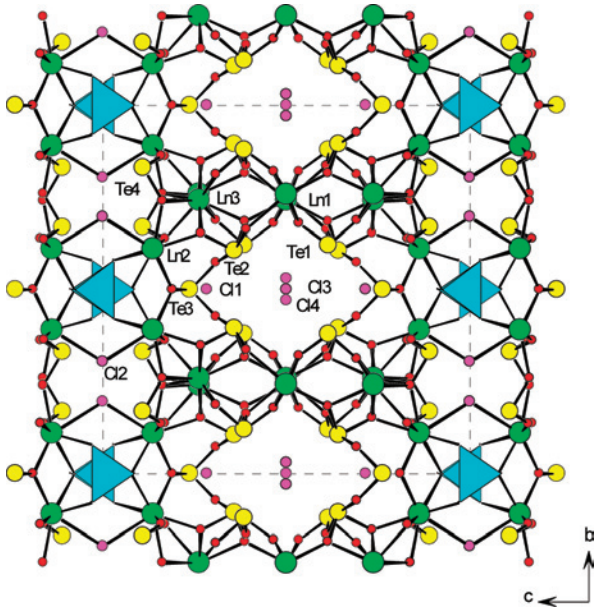

Figure 8. View of the structure of $Nd_5MoTe_7O_{23}Cl_3$ down the *a* axis. The MoO_4 tetrahedra are shaded in cyan. Nd, Te, Cl, and O atoms are drawn as green, yellow, pink, and red circles, respectively.

a distorted tetrahedral coordination environment with Mo−O distances in the range of 1.714(10)−1.845(9) Å. Te1, Te3, and Te4 are three-coordinated by three O atoms, whereas Te2 is four-coordinated. Two $Te1O_3$ groups, two $Te2O_4$ groups, and a $Te3O_3$ group are corner-sharing to form a novel $Te_5O_{13}^{6-}$ pentamer in a "semicycle" shape. The Te−O distances fall in the range of 1.845(8)−2.162(6) Å. The interconnection of Nd^{III} ions via $Te_5O_{13}^{6-}$ and TeO_3^{2-} anions resulted in a thick layer parallel to the *ab* plane. Neighboring lanthanide tellurium(IV) oxide layers are bridged by Cl2 atoms into a complicated 3D network, forming two different types of apertures (Figure 8). The MO_4 polyhedra are capped on both sides of the $Ln_4O_2Cl_2$ rings. The isolated Cl anions and the lone-pair electrons of Te^{IV} atoms of the $Te_5O_{13}^{6-}$ groups occupy the large apertures formed by eight-membered rings (Figure 8).

The solid-state luminescent properties of $Nd_2MoSe_2O_{10}$, $Nd_2MoTe_3O_{12}$, $Nd_2MoTe_4O_{14}$, and $Nd_2W_2Te_2O_{13}$ were investigated at both room temperature and 10 K, and the solid-state luminescent properties of $Nd_5MoTe_7O_{23}Cl_3$ and $Nd_5WTe_7O_{23}Cl_3$ were studied at room temperature. Under excitation at 514 nm, the room temperature emission spectra for all six Nd^{III} compounds display three sets of characteristic emission bands for the Nd^{III} ion in the near-IR region: $^4F_{3/2} \rightarrow {}^4I_{9/2}$, $^4F_{3/2} \rightarrow {}^4I_{11/2}$, and $^4F_{3/2} \rightarrow {}^4I_{13/2}$. $Nd_2MoTe_3O_{12}$ contains only one independent Nd^{III} site, whereas $Nd_2MoSe_2O_{10}$, $Nd_2MoTe_4O_{14}$, and $Nd_2W_2Te_2O_{13}$ each contain two unique Nd^{III} sites with C_1 symmetry. Because of the crystal-field effect, each transition band is expected to be split into several subbands. The $^4F_{3/2}$ is expected to split into two sublevels, whereas the complete degeneracy of $^4I_{9/2}$, $^4I_{11/2}$, and $^4I_{13/2}$ leads to five, six, and seven sublevels, respectively. Therefore, $^4F_{3/2} \rightarrow {}^4I_{9/2}$, $^4F_{3/2} \rightarrow {}^4I_{11/2}$, and $^4F_{3/2} \rightarrow {}^4I_{13/2}$ transitions will have a maximum of 10, 12, and 14 subbands if both the lower and upper levels of $^4F_{3/2}$ are populated as in the case of room temperature. When two and more unique Nd^{III} sites are present such as $Nd_2MoSe_2O_{10}$, $Nd_2MoTe_4O_{14}$, and $Nd_2W_2Te_2O_{13}$, the spectrum will be even more complicated. Because of the overlapping of some emission bands and resolution limit of the instruments, the observed emission peaks are usually fewer than that expected. At very low temperature such as 10 K, only the lower level of $^4F_{3/2}$ is populated; hence, the corresponding emission spectra are much simpler. Also the $^4F_{3/2} \rightarrow {}^4I_{11/2}$ transition, subbands are difficult to be resolved even at 10 K. The low-temperature emission spectrum for $Nd_2MoTe_3O_{12}$ displays five and six subbands for the $^4F_{3/2} \rightarrow {}^4I_{9/2}$ and $^4F_{3/2} \rightarrow {}^4I_{11/2}$ transitions, respectively, which is in good agreement with the theoretical expectation. Assuming the energy of the lowest sublevel of $^4I_{9/2}$ is 0 cm^{-1}, the energies of the lower level of $^4F_{3/2}$ and the other four sublevels for $^4I_{9/2}$ are calculated. Likewise, we can calculate the energies for the six sublevels of $^4I_{11/2}$. Upon excitation at 580 nm, both $Nd_2MoSe_2O_{10}$ and $Nd_2MoTe_4O_{14}$ display 8 and 10 subbands for the $^4F_{3/2} \rightarrow {}^4I_{9/2}$ and $^4F_{3/2} \rightarrow {}^4I_{11/2}$ transitions at 10 K, whereas $Nd_2W_2Te_2O_{13}$ displays eight and nine subbands at 10 K upon excitation at 288 nm. The lifetimes for the $^4F_{3/2} \rightarrow {}^4I_{11/2}$ transition were measured to be 0.21 and 0.20 ms and 3.2 and 3.6 μs respectively for $Nd_2MoSe_2O_{10}$ and $Nd_2MoTe_3O_{12}$ and for $Nd_2MoTe_4O_{14}$ and $Nd_2W_2Te_2O_{13}$. The three Pr^{III} compounds are capable of emitting luminescent light in the blue, green, and red regions. $Pr_5MoTe_7O_{23}Cl_3$ and $Pr_5WTe_7O_{23}Cl_3$ display four sets of emission bands at 491 nm (very strong, $^3P_0 \rightarrow {}^3H_4$), 534 nm (moderate, $^3P_0 \rightarrow {}^3H_5$), 619 nm (moderate, $^3P_0 \rightarrow {}^3H_6$), 649 nm (strong, $^3P_0 \rightarrow {}^3F_2$), and 735 nm (weak, $^3P_0 \rightarrow {}^3F_4$) under $\lambda_{ex} = 448$ nm. Under the same experimental conditions, the corresponding emission bands for $Pr_2MoTe_4O_{14}$ are much weaker. Because of the so-called "crystal-field effect" as well as multiple Pr^{3+} sites, a few transition bands were split into several subbands.[19]

3. $TM-d^0$ $TM-Te^{IV}$ or $Se^{IV}-O$ Systems. Reports on compounds in the $TM-Mo^{V}-Te^{IV}/Se^{IV}-O$ systems are much fewer than those of the alkali and alkaline-earth ones.[20] The structure of $Cd(VO_2)_4(SeO_3)_3 \cdot H_2O$ can be described as a pillared layered architecture. The layer is composed of dimers of VO_5 square pyramids and dimers of CdO_7 decahedra connected to one another by sharing corner and/or edge O atoms, whereas the pillars are composed of distorted VO_6 octahedra connected to one another via corner- and edge-sharing with capping selenite groups; the lone-pair electrons of the Se^{IV} atoms are oriented toward the long-narrow-shaped tunnels along the *b* axis.

We deem that the combination of the lone-pair electrons of Se^{IV} or Te^{IV} with the distorted MoO_6 octahedron may lead to new compounds in $TM-Mo^{VI}$ or $V^{V}-Se^{IV}/Te^{IV}-O$ systems with novel structures and unusual physical properties, such as magnetic or optical properties. So far, no nickel molybdenum(VI) selenite or tellurite has been structurally characterized. Our exploration of new phases in nickel

(20) Kim, Y.-T.; Kim, Y.-H.; Park, K.; Kwon, Y.-U.; Young, V. G., Jr. *J. Solid. State Chem.* **2001**, *161*, 23.
(21) Jiang, H. L.; Xie, Z.; Mao, J. G. *Inorg. Chem.* **2007**, *46*, 6495.

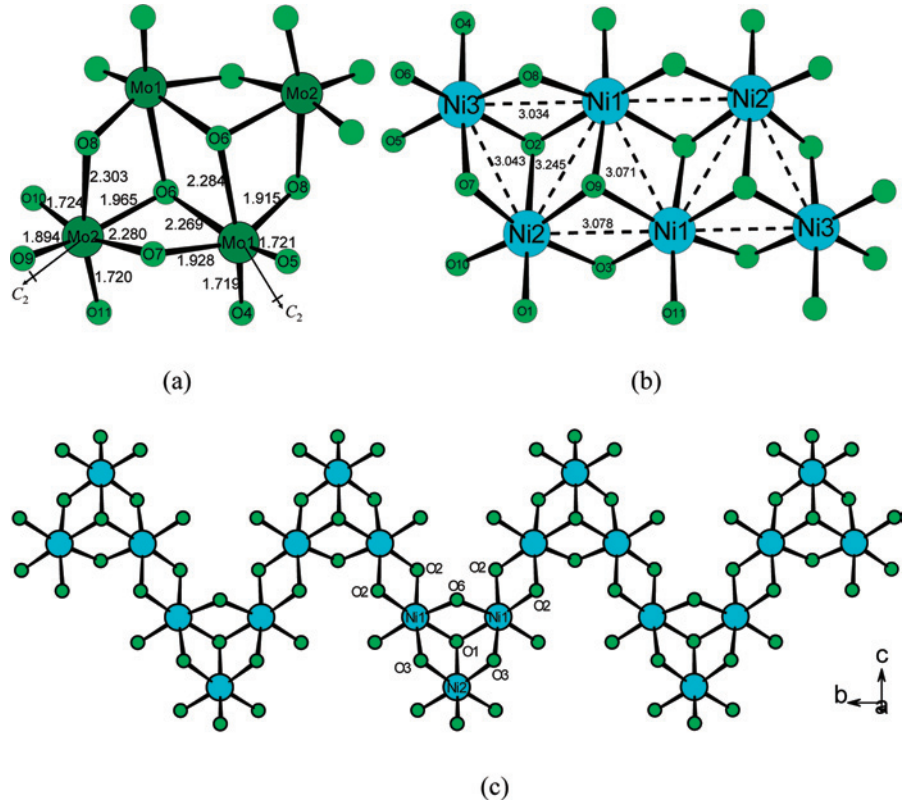

Figure 9. $[Mo_4O_{16}]^{8-}$ tetranuclear cluster unit (a) and $[Ni_6O_{22}]^{32-}$ hexanulear cluster unit in $Ni_3(Mo_2O_8)(SeO_3)$ (b), and 1D $[Ni_3O_{11}]^{16-}$ corrugated chain along the *b* axis in $Ni_3(Mo_2O_8)(TeO_3)$ (c).

molybdenum(VI) selenite or tellurite systems led to three new compounds, namely, $Ni_3(Mo_2O_8)(XO_3)$ (X = Se, Te)[21] and $Ni_3(MoO_4)(TeO_3)_2$.[22]

$Ni_3(Mo_2O_8)(XO_3)$ (X = Se, Te) display two different types of 3D structures containing $[Mo_4O_{16}]^{8-}$ and $[Ni_6O_{22}]^{32-}$ clusters or 1D nickel oxide chains (Figure 9). The structure of $Ni_3(Mo_2O_8)(SeO_3)$ features a 3D network in which $[Ni_6O_{22}]^{32-}$ cluster units are interconnected by $[Mo_4O_{16}]^{8-}$ clusters and SeO_3^{2-} anions. All three Ni^{II} ions in the asymmetric unit are octahedrally coordinated by six O atoms, with Ni−O distances ranging from 1.983(4) to 2.160(4) Å. Both Mo^{VI} cations are octahedrally coordinated by six O atoms. The Mo−O bond distances are in the range of 1.719(4)−2.304(4) Å. The Mo^{VI} cations are distorted toward an edge (local C_2 direction) with two "short", two "normal", and two "long" Mo^{6+}−O bonds. The magnitudes of the distortions (Δ_d) were calculated to be 1.18 and 1.29 Å respectively for Mo1 and Mo2. The four $Mo^{VI}O_6$ octahedra are interconnected by edge-sharing to form a cyclic $[Mo_4O_{16}]^{8-}$ tetranuclear cluster unit (Figure 9a). Six NiO_6 octahedra are interconnected into a hexanuclear $[Ni_6O_{22}]^{32-}$ cluster unit through edge-sharing (Figure 9b). The intracluster Ni···Ni separations between a pair of edge-sharing NiO_6 octahedra are in the range of 3.034(1)−3.245(1) Å (Figure 9b). The $[Ni_6O_{22}]^{32-}$ cluster units are bridged by SeO_3^{2-} groups to form a 2D nickel selenite layer parallel to the *ab* plane. Neighboring nickel selenite layers are further interconnected by the $[Mo_4O_{16}]^{8-}$ clusters via Mo−O−Ni bridges into a 3D network structure. The lone-pair electrons of the Se^{IV} atoms are oriented toward the cavities of the structure. The structure of $Ni_3(Mo_2O_8)(TeO_3)$ is different from that of $Ni_3(Mo_2O_8)(SeO_3)$, although their chemical formulas are comparable. It features a 3D structure in which the corrugated nickel oxide anionic chains are bridged by $[Mo_4O_{16}]^{8-}$ cluster units and TeO_3^{2-} anions. As in $Ni_3(Mo_2O_8)(SeO_3)$, the Ni^{II} and Mo^{VI} cations are octahedrally coordinated by six O atoms. Similar to that in $Ni_3(Mo_2O_8)(SeO_3)$, the four $Mo^{VI}O_6$ octahedra in $Ni_3(Mo_2O_8)(TeO_3)$ are interconnected via edge-sharing to form a $[Mo_4O_{16}]^{8-}$ tetranuclear cluster unit. Two $Ni1O_6$ and one $Ni2O_6$ octahedra are interconnected via edge-sharing into a $[Ni_3O_{13}]^{20-}$ trinuclear unit. Such neighboring trinuclear units are further interconnected through edge-sharing into a corrugated $[Ni_3O_{11}]^{16-}$ anionic chain along the *b* axis with a Ni1−O2−Ni1 bond angle of 84.65(9)° (Figure 9c). This nickel oxide chain can also be viewed as $Ni2O_6$ octahedra being grafted onto the corrugated chain of $Ni1O_6$ through edge-sharing. It is interesting to note that $[Ni_6O_{22}]^{32-}$ clusters are formed in $Ni_3(Mo_2O_8)(SeO_3)$, whereas corrugated $[Ni_3O_{11}]^{16-}$ anionic chains are observed in $Ni_3(Mo_2O_8)(TeO_3)$. Both nickel oxide building units are based on Ni_3O triangles. The Ni_3O triangles in $[Ni_6O_{22}]^{32-}$ clusters are condensed via sharing Ni−Ni edges, whereas those in $[Ni_3O_{11}]^{16-}$ anionic chains are interconnected through pairs of Ni−O−Ni bridges. These different nickel(II) oxide architectures may result from the different coordination modes of the selenite and tellurite groups as well as the different ionic radii of Se^{IV} and Te^{IV}. Neighboring corrugated nickel(II) oxide chains are bridged by TeO_3^{2-} anions to form a thick nickel(II) tellurite layer parallel to the *ab* plane. The

(22) Jiang, H. L.; Mao, J. G. Unpublished results.

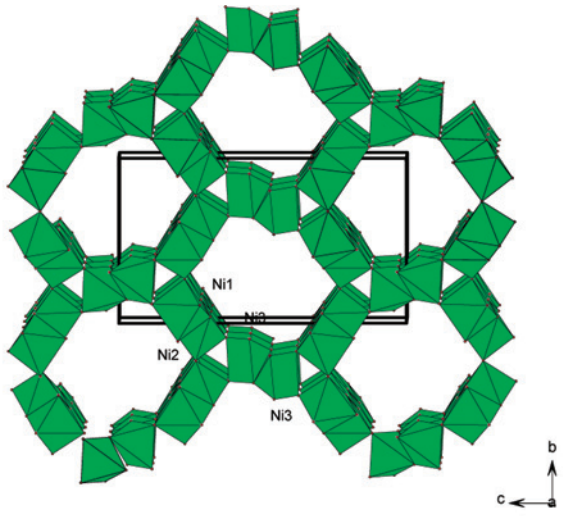

(a)

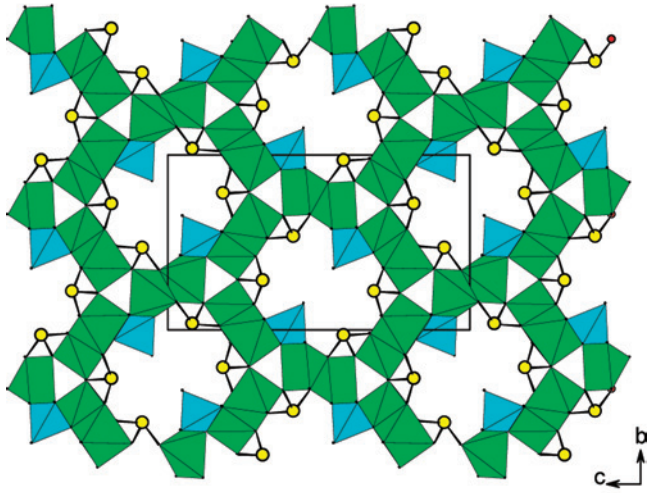

(b)

Figure 10. 3D network of nickel(II) oxide in $Ni_3(MoO_4)(TeO_3)_2$ (a) and view of the structure of $Ni_3(MoO_4)(TeO_3)_2$ along the *a* axis. The NiO_6 and NiO_5 polyhedra are shaded in green, and MoO_4 tetrahedra are shaded in cyan. Te atoms are drawn as yellow circles.

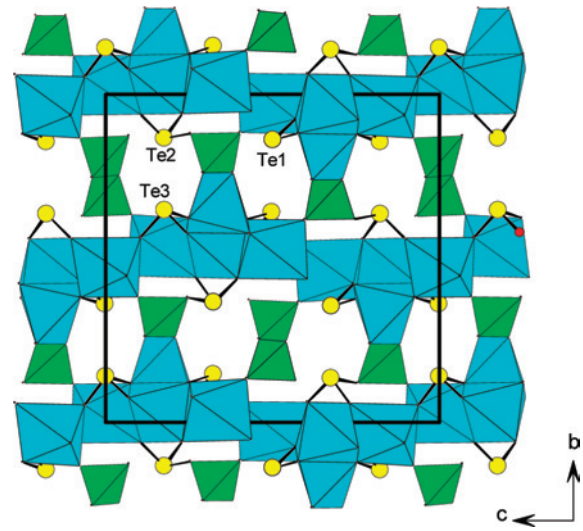

Figure 11. View of the structure of $Cd_4V_2Te_3O_{15}$ down the *a* axis. The CdO_6 and VO_4 polyhedra are shaded in blue and green, respectively. Te and O atoms are drawn as yellow and red circles, respectively.

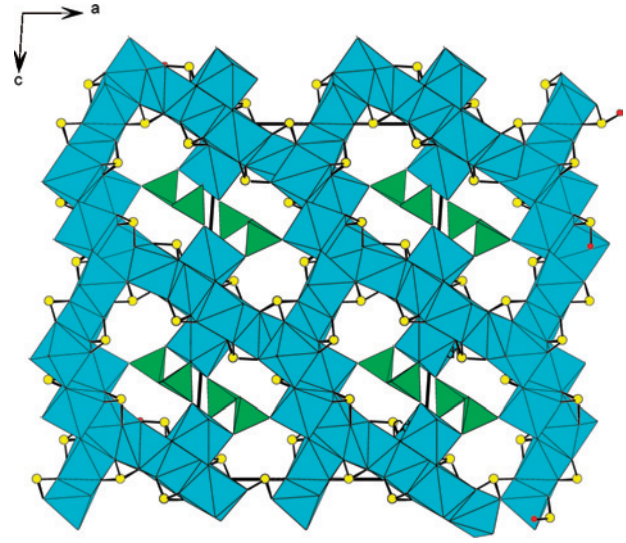

Figure 12. View of the structure of $Cd_6V_2Se_5O_{21}$ down the *b* axis. The CdO_6, CdO_7 and CdO_8 polyhedra are shaded in cyan and VO_4 tetrahedra in green. Se and O atoms are drawn as pink and red circles, respectively.

thickness of the layer is about 12.1 Å. Such layers are further interconnected by the $[Mo_4O_{16}]^{8-}$ clusters via Mo−O−Ni bridges into a 3D network structure. The lone-pair electrons of the Te^{IV} atoms are oriented toward the tunnels of the structure.

When we increased the molar ratio of TeO_2/MoO_3 to 2:1, a new Ni−Mo−Te−O phase with NCS structure (space group $P2_12_12_1$), $Ni_3(MoO_4)(TeO_3)_2$, was obtained recently.[22] Its structure features a novel 3D network of nickel(II) oxide with larger 1D tunnels along the *a* axis. The MoO_4 tetrahedra and TeO_3 groups cap the walls of the tunnels (Figure 10). Among three unique Ni^{II} ions in the asymmetric unit, two are octahedrally coordinated, whereas the third one is in a square-pyramidal geometry. NiO_6 octahedra are interconnected by edge-sharing along the *a* axis into a 1D chain, whereas NiO_5 polyhedra are corner-sharing along the *a* axis into a 1D chain. These two types of chains are further interconnected via corner-sharing into a 3D open framework of nickel oxide, forming 1D helical tunnels along the *a* axis, which are based on Ni_{12} rings (Figure 10a). Unlike those in $Ni_3(Mo_2O_8)(SeO_3)$ and $Ni_3(Mo_2O_8)(TeO_3)$, the Mo^{VI} cation is in a tetrahedral environment and there are no Mo−O−Mo or Mo−O−Te bridges. The MoO_4 tetrahedra and TeO_3 groups cap walls of the tunnels; the lone-pair electrons of Te^{IV} cations and terminal O atoms of the MoO_4 tetrahedra are pointing toward the center of the tunnel (Figure 10b). SHG measurements indicate that its SHG signal is very weak.

Both $Ni_3(Mo_2O_8)(SeO_3)$ and $Ni_3(Mo_2O_8)(TeO_3)$ obey the Curie−Weiss law above 60 K with Weiss constants (θ) of 15.4(2) and 5.5(1) K respectively for Se and Te compounds, indicating significant ferromagnetic interactions between

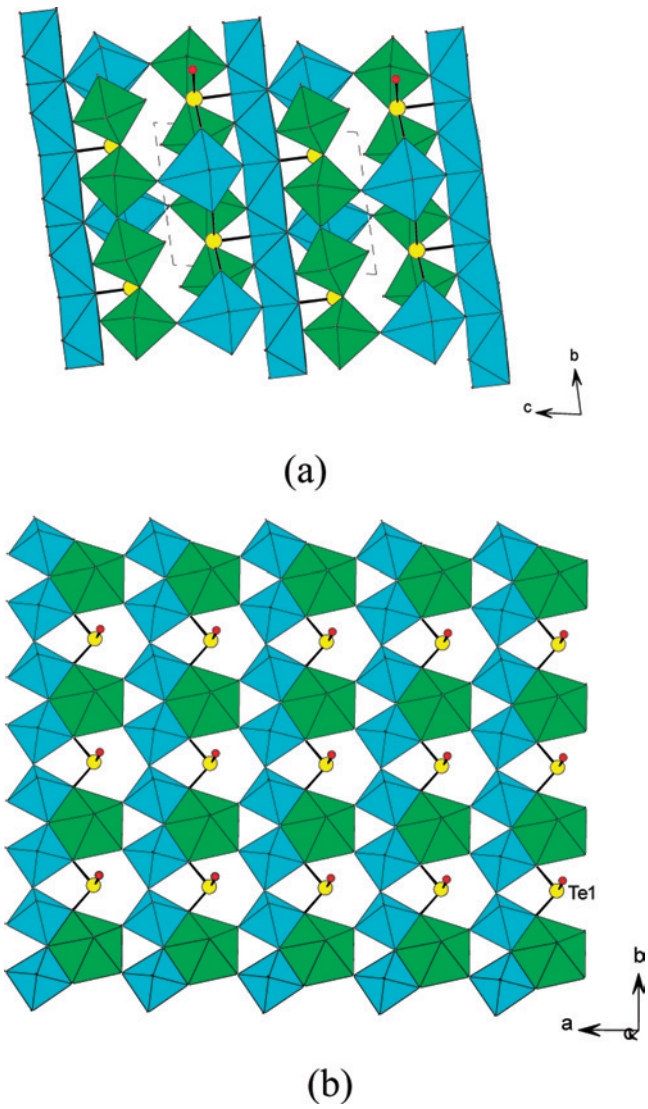

Figure 13. View of the structure of $CdWTeO_6$ down the *a* axis (a) and a 2D layer composed of $Cd2O_7$, WO_6, and $Te1O_3$ groups (b). The CdO_6 and CdO_7 polyhedra are shaded in green and the WO_6 octahedra in green. Te and O atoms are drawn as yellow and red circles, respectively.

magnetic centers. It is expected that the magnetic interactions should be dominated by the magnetic interactions between Ni^{II} ions within the hexanuclear $[Ni_6O_{22}]^{32-}$ cluster in $Ni_3(Mo_2O_8)(SeO_3)$ and the 1D $[Ni_3O_{11}]^{16-}$ anionic chain in $Ni_3(Mo_2O_8)(TeO_3)$. Long-range magnetic ordering is observed below 28 and 56 K.

We also extended our studies to TM ions with a d^{10} electronic configuration such as Zn^{II} and Cd^{II} ions.[23] Zn^{II} or Cd^{II} compounds may display semiconducting properties, and they are also able to emit blue light. Solid-state reactions of zinc(II) or cadmium(II) oxide, V_2O_5 and TeO_2, at high temperature lead to two novel quaternary compounds, namely, $Zn_3V_2TeO_{10}$ and $Cd_4V_2Te_3O_{15}$.[23] Very recently $Cd_6(V_2O_6)(SeO_3)_5$ and $CdWTeO_6$ were also isolated.[24]

The structure of $Zn_3V_2TeO_{10}$ is a complicated 3D network constructed by the interconnection of ZnO_5, ZnO_6, VO_4, and

(23) Jiang, H.-L.; Huang, S.-P.; Fan, Y.; Mao, J.-G.; Cheng, W.-D. *Chem.—Eur. J.* **2008**, *14*, 1972.

(24) (a) Jiang, H. L.; Kong, F.; Fan, Y.; Mao, J.-G. *Inorg. Chem.* **2008**, *47*, ASAP paper. (b) Jiang, H. L.; Mao, J. G. Unpublished results.

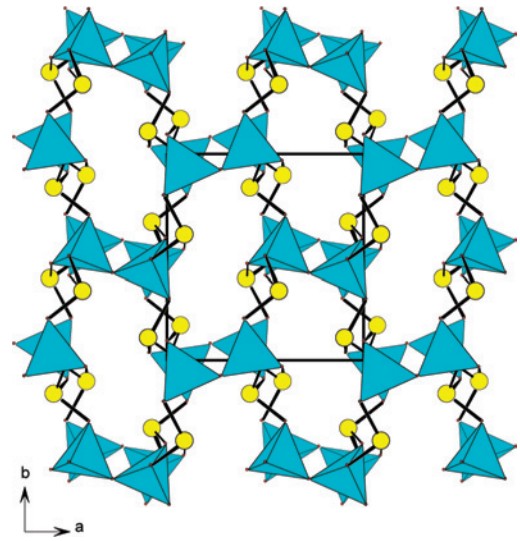

Figure 14. View of the structure of $Se_2B_2O_7$ down the *b* axis. BO_4 tetrahedra are shaded in cyan. Se, B, and O atoms are drawn as yellow, cyan, and red circles, respectively.

TeO_4 polyhedra via corner- and edge-sharing. $Cd_4V_2Te_3O_{15}$ with an acentric structure features a 3D network in which the cadmium tellurite layers are further interconnected by both "isolated" VO_4 tetrahedra and 1D vanadium oxide helical chains (Figure 11). $Cd_4V_2Te_3O_{15}$ displays a SHG efficiency of about 1.4 times that of KDP. It is stable up to 840 °C and shows little absorption in 0.6−10.0 μm. Luminescent measurements indicate that both compounds exhibit broad emission bands in the blue-light region.[23]

$Cd_6V_2Se_5O_{21}$ was obtained by solid-state reactions of cadmium(II) oxide, V_2O_5 and SeO_2. Its structure is composed of a 3D open framework of cadmium(II) selenite and 1D vanadium(V) oxide chains of corner-sharing VO_4 tetrahedra. The vanadium(V) oxide chains are inserted at the large tunnels of cadmium(II) selenite via V−O−Cd bridges. The Cd^{II} ions are coordinated by six, seven, or eight O atoms (Figure 12).[24a] $CdWTeO_6$ crystallized in triclinic $P\bar{1}$; its structure features a complicated 3D network of corner/edge-sharing CdO_6 octahedra, CdO_7 pentagonal bipyramids, WO_6 octahedra, and TeO_3 groups (Figure 13). There are three Cd^{II}, two W^{VI}, and two Te^{IV} sites in its asymmetric unit. Two Cd^{II} sites lying on the center of symmetry are octahedrally coordinated, and the third Cd^{II} ion in a general position is seven-coordinated in a pentagonal-bipyramidal geometry. The CdO_6 octahedra form 1D chains along the *b* axis via edge-sharing; these 1D chains are capped by $Te2O_3$ groups. The WO_6 octahedra are distorted toward a face (local C_3 direction). Neighboring WO_6 octahedra are interconnected via corner-sharing into 1D chains also along the *b* axis. These tungsten oxide chains are further capped by $Te2O_3$ groups on one side, and they are further bridged by CdO_7 polyhedra via edge- and corner-sharing into a 2D layer parallel to the *ab* plane (Figure 13b). Two such layers are interconnected into a double layer via Cd−O−W bridges. The above two types of building units are alternating and interconnected along the *c* axis via corner-sharing (Te−O−Cd, Cd−O−W, and Cd−O−Cd bridges) into a 3D architecture (Figure 13a).[24b]

Part II. Metal Tellurites and Selenites Containing Tetrahedral Groups of Main-Group Elements

So far such compounds are still rare. With respect to tellurite phosphate oxides, a few materials have been reported, namely, $Te_2O_3(HPO_4)$, $Te_8O_{10}(PO_4)_4$, $Ba_2TeO(PO_4)_2$, $BaTeMO_4(PO_4)$ ($M = Nb^{5+}$ or Ta^{5+}), and $A_2TeMo_2O_6(PO_4)_2$ (A = K, Rb, Cs, Tl).[25] Structurally these materials are different; $BaNbTeO_4(PO_4)$ contains 2D layers, whereas $Te_2O_3(HPO_4)$ and $Te_8O_{10}(PO_4)_4$ exhibit 3D structures consisting of asymmetric TeO_4 and TeO_5 polyhedra that are linked through corner-sharing.[25a–c] $Ba_2TeO(PO_4)_2$ displays a novel 1D chain structure that is composed of PO_4 tetrahedra and TeO_5 polyhedra. Te^{4+} cations are in asymmetric coordination environments attributable to their lone pairs. Two TeO_5 polyhedra form a dimeric unit via edge-sharing; two neighboring Te_2O_8 units are further interconnected via a pair of phosphate groups into a 1D chain along the *b* axis, and each Te^{IV} atom is also bonded to the third phosphate group through one Te−O−P bridge.[25d] The isostructural mixed-metal phosphates, $BaMTeO_4(PO_4)$ ($M = Nb^{5+}$, Ta^{5+}), have novel layered crystal structures consisting of M^VO_6 corner-sharing octahedral chains that are connected to $Te^{IV}O_4$ polyhedra and phosphate tetrahedra. The phosphate groups act as pendent groups between two neighboring layers. The Nb^{5+} cation distorts along the local C_4 direction of its octahedron with a "short−long−short−long" Nb−O−Nb bond motif. Furthermore, the Nb^{5+} cation displaces away from the oxide ligands that are bonded to Te^{4+} or P^{5+} cations, attributable to the structural rigidity of the TeO_4 and PO_4 polyhedra.[25e] $A_2Mo_2TeO_6(PO_4)_2$ displays a pillared layered architecture composed of $Mo_2P_2O_{14}$ layers and TeO_4 groups as the pillars. Within the $Mo_2P_2O_{14}$ layer, the MoO_6 octahedra (distorted toward an edge) and PO_4 tetrahedra are interconnected via corner-sharing, forming Mo_2P_2 four-membered rings and Mo_4P_4 eight-membered rings.[25f]

So far, there is no reports on metal selenites or tellurites containing additional SiO_4 or GeO_4 tetrahedra. Our exploration into the unexplored RE−Ge/Si−Te^{IV}−O systems afforded two novel lanthanum(III) tellurites with additional SiO_4 or GeO_4 tetrahedra, namely, $La_4(Si_{5.2}Ge_{2.8}O_{18})(TeO_3)_4$ and $La_2(Si_6O_{13})(TeO_3)_2$.[26]

The structure of $La_4(Si_{5.2}Ge_{2.8}O_{18})(TeO_3)_4$ features a 3D network composed of the $[(Si_{5.2}Ge_{2.8})O_{18}]^{4-}$ tetrahedral layers and the $[La_4(TeO_3)_4]^{4+}$ layers that alternate along the *b* axis. The germanate−silicate layer consists of corner-sharing XO_4 (X = Si, Ge) tetrahedra, forming four- and six-membered rings. The structure of $La_2(Si_6O_{13})(TeO_3)_2$ is a 3D network composed of the $[Si_6O_{13}]^{2-}$ double layers and the $[La_2(TeO_3)_2]^{2+}$ layers that alternating along the *a* axis. The $[Si_6O_{13}]^{2-}$ double layer is built by corner-sharing silicate tetrahedra, forming four-, five-, and eight-membered rings. The TeO_3^{2-} anions in both compounds are only involved in the coordination with the La^{3+} ions to form a lanthanum(III) tellurite layer.[26]

We also developed a new SHG material, $Se_2B_2O_7$, by the combination of BO_4 tetrahedra with SeO_3^{2-} groups.[27] The structure of $Se_2B_2O_7$ features a 3D network composed of dimers of corner-sharing BO_4 tetrahedra and SeO_3 groups (Figure 14). The open framework of $Se_2B_2O_7$ can also be described as an interesting mixed (3,4)-connected net of the B and Se atoms (linked by −O− bridges). Right-handed helical tunnels along the *c* axis are formed. These tunnels are based on B_6Se_4 10-membered rings. The lone pairs of the Se^{IV} cations are oriented toward the above tunnels. $Se_2B_2O_7$ is stable up to 300 °C. It exhibits a SHG efficiency of about 2.2 times that of KDP (KH_2PO_4). $Se_2B_2O_7$ is transparent in the range of 300−2000 nm, and it exhibits an optical band gap of 4.64 eV.[27]

Conclusions and Outlook

Several factors have strong effects on the structural topologies of the resulting compounds. The slight change of the ionic radius of the cation such as the A^I or Ln^{III} ion could lead to a completely different structure such as, for example, $A_2W_3TeO_{12}$ ($A = K^+$, Rb^+, Cs^+)[12c] and $Ln_2MoTe_3O_{12}$ (Ln = La, Nd).[19a] Also metal tellurites usually show structures different from the corresponding selenites because of the larger ionic radius of Te^{IV} than Se^{IV}, such as, for example, $Ni_3(Mo_2O_8)(QO_3)$ (Q = Se, Te).[21] In some cases, isomerism exists for some metal tellurites. Recently, we obtained a cubic phase of $Ga_2Te_3O_9$ ($I\bar{4}3d$) and a hexagonal phase of $Ga_2Te_3O_9$ ($P6_3/m$) in the same hydrothermal reaction; the cubic phase is SHG active (1 × KDP) and is densely packed, whereas the centrosymmetric hexagonal phase has a much lower density and features a 3D network with large tunnels along the *c* axis.[28] Molar ratios of the starting materials, synthetic methods, and reaction temperatures are also very important factors.

Several trends are obvious. The combination of the two types of cations susceptible to SOJT distortion, d^0 TM and lone-pair cation (Te^{IV} or Se^{IV}), not only gives rise to a rich structural chemistry but also affords many NCS compounds with good SHG properties. As for the direction of the out-of-center distortion, it was found that V^{5+} and Nb^{5+} usually displace toward an edge or corner, whereas Mo^{6+} and W^{6+} ions are more likely distorted toward an edge or face. The V^{5+} cation may adopt the square-pyramidal geometry besides a tetrahedron and a octahedron. Also it is not as stable as other d^0 TM cations, and sometimes it is reduced to V^{4+} during the reaction. The bond polarization follows the following order: $Te^{IV} > Se^{IV}$ and $Mo^{6+} > V^{5+} > W^{6+} > Nb^{5+} > Ta^{5+}$.[2] It is observed that Ln^{III} compounds are seldom acentric and the d^0 TM cations are more likely tetrahedrally coordinated; this may be due to the higher coordination number for the Ln^{III} ions than the A^I and AE^{II} cations. It is

(25) (a) Mayer, H. *Z. Kristallogr.* **1975**, *141*, 354. (b) Alcock, N. W.; Harrison, W. D. *Acta Crystallogr.* **1982**, *38*, 1809. (c) Mayer, H.; Pupp, G. *Z. Kristallogr.* **1977**, *145*, 321. (d) OK, K.-M.; Halasyamani, P. S. *J. Solid. State Chem.* **2006**, *179*, 1345. (e) Ok, K.-M.; Orzechowski, J.; Halasyamani, P. S. *Inorg. Chem.* **2004**, *43*, 964. (f) Guesdon, A.; Raveau, B. *Chem. Mater.* **2000**, *12*, 2239.

(26) Kong, F.; Jiang, H.-L.; Mao, J.-G. *J. Solid State Chem.* **2008**, *181*, 263.

(27) Kong, F.; Huang, S.-P.; Sun, Z.-M.; Mao, J.-G.; Cheng, W.-D. *J. Am. Chem. Soc.* **2006**, *128*, 7750.

(28) Kong, F.; Mao, J. G. Unpublished results.

worth mentioning that the Se^{IV} cation exists mostly as a SeO_3 group (in some cases as the diselinite group),whereas Te^{IV} can be three-, four-, or five-coordinated, and the most amazing aspect is that these TeO_x ($x = 3-5$) polyhedra can be polymerized into many types of polynuclear clusters or extended skeletons (Scheme 1) besides a ditellurite anion; such a polymerization is hardly observed in the organically templated or organically covalently bonded metal tellurites. Inorganic solids with various polymeric tellurium(IV) oxide anions include a $Te_3O_8^{4-}$ trimer in $La_2MoTe_3O_{12}$, a $Te_4O_{11}^{6-}$ tetramer in $Er_2Te_4O_{11}$,[29] a $Te_5O_{13}^{6-}$ pentamer in $Ln_5MTe_7O_{23}Cl_3$ (Ln = Pr, Nd; M = Mo, W), a 1D $Te_4O_{10}^{4-}$ in $Ln_2MoTe_4O_{14}$ (Ln = Pr, Nd), a 1D $Te_6O_{13}^{2-}$ in $\{Cd_2(Te_6O_{13})\}\{Cd_2Cl_6\}$, a 1D $Te_7O_{17}^{6-}$ in $Cd_7Cl_8(Te_7O_{17})$, layered $Te_3O_7^{2-}$ in $La_2WTe_6O_{18}$, a 2D $Te_4O_9^{2-}$ in $K_2Te_4O_9 \cdot 3.2H_2O$,[30a] and a 2D $Te_2O_5^{2-}$ in $Ln(Te_2O_5)X$ (Ln = Nd, X = Cl, Br; Ln = Gd, X = Cl).[30b,c] Certainly more examples will be discovered in the future, and extensive theoretical studies are needed to understand its origin.

There are also many fertile lands for our exploration in the field of metal selenites and tellurites. Systematic investigation on the $Ln^{III}-V^{5+}$ (Nb^{5+}, Ta^{5+}, Ti^{4+})$-Te^{IV}$ (or Se^{VI})$-O$ systems is expected to afford many compounds with new structural types as well as excellent luminescent materials. The mixing of two types of charge-balancing cations such as Ln−AE, AE−A, and Ln−A could change the overall charges of the anionic networks in addition to breaking the packing limitation for the single-type cation; thus, a variety of new structures can be obtained. The combination of lone-pair Te^{IV} or Se^{IV} with borate is also quite promising in the search for new SHG materials. In order to exhibit good second-order NLO properties, the above two types of bond polarizations should be "adductive", which is still a great challenge for a synthetic chemist. To fully address these problems, strong interactions between synthetic and theoretical chemists are necessary.

Acknowledgment. This work was supported by the National Natural Science Foundation of China (Grants 20731006, 20573113, and 20521101).

IC8005629

(29) Shen, Y.-L.; Mao, J.-G. *J. Alloys Compd.* **2004**, *385*, 86.
(30) (a) Ok, K. M.; Halasyamani, P. S. *Chem. Mater.* **2001**, *13*, 4278. (b) Nikiforov, G. B.; Kusainova, A. M.; Berdonosov, P. S.; Dolgikh, V. A.; Lightfoot, P. *J. Solid State Chem.* **1999**, *146*, 473. (c) Meier, S. F.; Schleid, T. *Z. Anorg. Allg. Chem.* **2003**, *629*, 1575.